Correction of Eddy Currents in EPI-based Diffusion Tensor Imaging

Aziz Hatim Poonawalla[1], Xiaohong Joe Zhou[1]
[1]University of Texas M.D. Anderson Cancer Center, 1515 Holcombe Boulevard, Box 57, Houston, TX USA;

Introduction

Echo-planar imaging (EPI) is commonly used in diffusion-weighted imaging (DWI) and diffusion-tensor imaging (DTI), primarily because of its speed and motion-insensitivity. In diffusion EPI pulse sequences, the strong diffusion-weighting gradient and the rapid slew rate (required to minimize TE) can produce substantial eddy currents, leading to image artifacts. Conventional eddy current-compensation techniques using pre-emphasis are often inadequate to eliminate the artifacts. The artifacts in DWI have been well characterized (1,2), and several correction techniques have been described (1-5). However, the effect of eddy currents on DTI and the effectiveness of the proposed correction methods have not been systematically investigated. Towards this end, we report observation of several artifacts caused by residual eddy currents in DTI, and the efficacy of a method to reduce the eddy current induced errors by modifying the receiver phase/frequency and the imaging gradients in real-time (5).

Effects of Eddy Currents

The eddy currents induced by a diffusion-weighting gradient used in EPI produce a time-dependent magnetic field. To a first-order approximation, this field can be decomposed into a spatially constant field $b_0(t)$ and three linear gradient fields, $g_x(t)$, $g_y(t)$, and $g_z(t)$ (5). These spatial components can be characterized by:

$$b_{m0}(t) = \sum_j \alpha_{m0j} R\tau_{m0j} C(\tau_{m0j}) e^{-t/\tau_{m0j}} \qquad [1]$$

$$g_{mn}(t) = \sum_j \alpha_{mnj} R\tau_{mnj} C(\tau_{mnj}) e^{-t/\tau_{mnj}} \qquad [2]$$

where m is the axis of the applied diffusion-weighting gradient, and n the axis of the affected spatial-encoding gradient (m, n $\in$ { x, y, z}). The quantities α_{mnj} and τ_{mnj} are the amplitude and time constant, respectively, of the j^{th} eddy current component. $C(\tau)$ is a function of τ, as well as the timing parameters of the diffusion-weighting gradients. R is the slew rate. In DWI, these errors manifest as three kinds of image artifacts: distortion (compression and shear), shift, and image intensity loss (2).

DTI involves mathematical manipulation of raw diffusion-weighted images to create various maps of derived quantities, such as relative anisotropy and principal eigenvectors. The extensive computational chain can cause the eddy current induced artifacts to manifest differently in DTI than in DWI.

The shear, compression, and shift observed in DWI result in two types of artifacts in DTI: hyper-intense regions which appear as false fiber tracts, and reduced resolution due to blurring. The other prevalent eddy current induced DTI artifact is an enhancement of the background intensity, which stems from the inconsistent signal loss in the raw DWI data. We observed these artifacts in our studies on water phantoms and human subjects. The eddy current-induced artifacts are of particular concern when diffusion-tensor images are used for pre-surgical planning of brain tumors and tissue characterization (6,7).

Correction Methods

A correction technique, previously implemented in a DWI pulse sequence (5), was adapted to a DTI sequence based on EPI. We performed all EPI experiments (both DWI and DTI) on a GE Signa EchoSpeed 1.5 T MR scanner (GE Medical Systems, Milwaukee, WI) with TR = 4 sec, TE = 98 msec, FOV = 24 cm, b = 1000 s/mm^2, matrix = 128^2, and slice thickness = 5 cm.

The correction technique was a three-stage process performed using a water phantom. First, we determined the residual eddy current amplitudes (α_{mn}) and time constants (τ_{mn}) empirically by acquiring DWI data, with diffusion gradients sequentially applied along the three orthogonal axes {x, y, z} to isolate the eddy current effects induced by each physical gradient axis. Second, we used the amplitudes (α_{mn}) and time constants (τ_{mn}) to calculate the error terms for the DTI pulse sequence according to Equations [1] and [2]. Third, we input the compensation terms into the DTI pulse sequence in real-time. The pulse sequence modified the receiver phase/frequency and imaging gradients accordingly to compensate for the eddy current effects (5).

After the phantom experiments, we acquired two diffusion-tensor data sets on a human volunteer, one with and one without the eddy current-compensation scheme enabled. Both data sets were acquired at b = 1000 s/mm^2 using six diffusion-weighted gradients (8). All other acquisition parameters were identical to the calibration phantom studies. Relative diffusion anisotropy maps were then generated from each data set for comparison.

Results and Discussion

Figure 1 illustrates two diffusion-tensor images before (left) and after (right) applying the eddy current correction technique. With the correction, the hyper-intense regions at the margins are considerably reduced. The compensation method also decreased the intensity from tissues with more isotropic diffusion, such as gray matter.

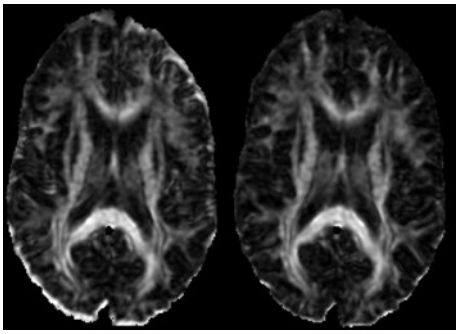

Figure 1. Two diffusion-tensor images (relative diffusion anisotropy maps) which illustrate the effectiveness of the eddy current correction technique (*left*: without correction; *right*: with correction).

In DTI, eddy currents arising from the diffusion-weighting gradients can produce artifacts, including false fiber tracks, enhanced background, and image blurring. These artifacts can be effectively reduced with the proposed correction method. The compensation parameters can be determined empirically using a phantom for a given acquisition protocol. For maximum efficiency, however, the compensation parameters should be determined automatically and cover a broader range of acquisition parameters. Although system-level approaches to eddy current error reduction and compensation are preferable, the correction method described herein provides an alternative to effectively reduce image artifacts in DTI.

References

1. Jezzard et. al., *Magn. Reson. Med.*, 39:801-12 (1998).
2. Zhou et al., *Proc. 5th Int'l. Soc. Magn. Reson. Med.*, pg.1722 (1997).
3. Reese et. al., *Proc. 6th Int'l. Soc. Magn. Reson. Med.*, pg.663 (1998).
4. Heid, *Proc. 8th Int'l. Soc. Magn. Reson. Med.*, pg.799 (2000).
5. Zhou et al, US Patent, 5,770,934, June 23 (1998).
6. Zhou et. al., *Proc. 8th Int'l. Soc. Magn. Reson. Med.*, pg.480 (2000).
7. Basser, *NMR in Biomed.*, 8:333-44 (1995).
8. Basser, *Magn. Reson. Med.*, 39:928-34 (1998).